Charged particle distributions and correlations in p+p collisions measured with the ATLAS detector

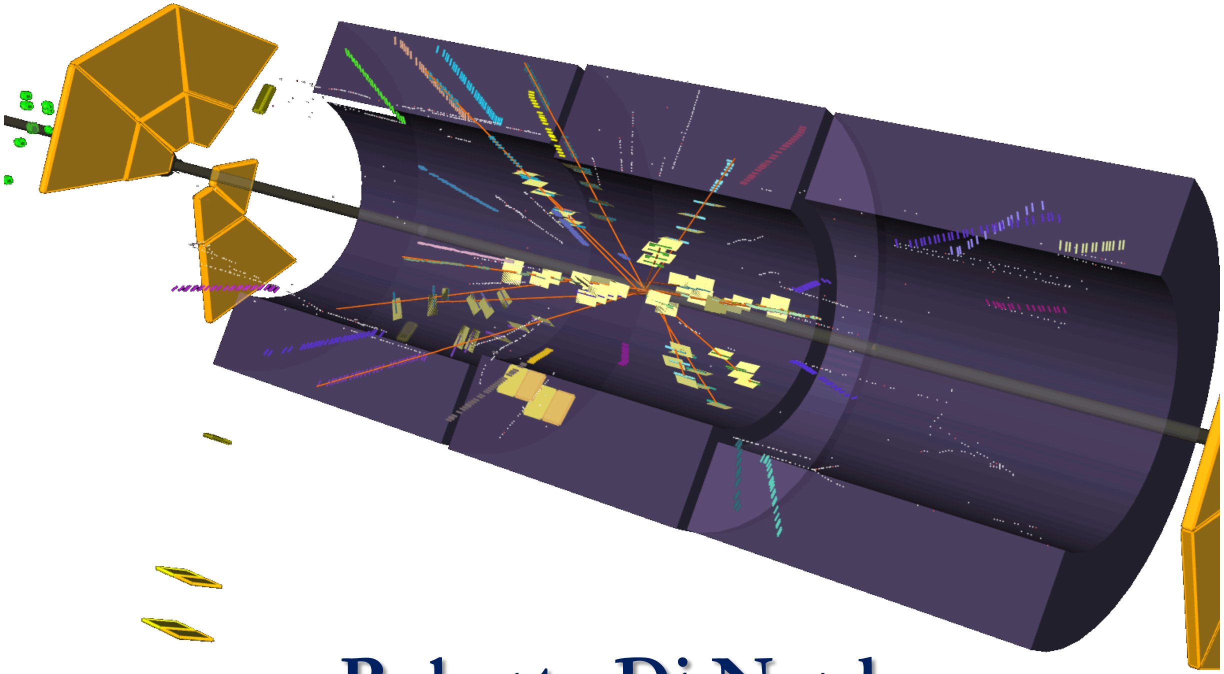

Roberto Di Nardo

University & INFN Roma Tor Vergata,

On behalf of the ATLAS Collaboration

6th International Workshop High-pT physics at LHC 2011
4-7 April 2011, Utrecht, Netherlands

Outline

- The ATLAS experiment and the Inner Detector
    - Reconstruction of known particles in Minimum Bias Events
- Charged particle multiplicity spectra
- Underlying event measurements
- Two-particle angular correlation

Roberto Di Nardo – University & INFN Tor Vergata

Motivations

$$\sigma_{tot} = \sigma_{EL} + \sigma_{ND} + \sigma_{SD} + \sigma_{DD}$$

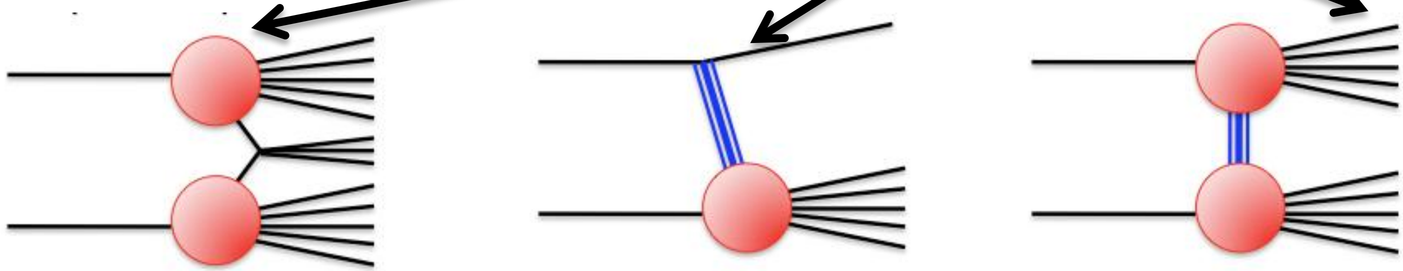

Non-Diffractive (~49 mb) @7TeV | Single-Diffractive (~14 mb) @7TeV | Double-Diffractive (~9 mb) @7TeV

- Soft QCD processes are unavoidable background for a lot of collider observables (in particular jet cross-section, missing energy, isolation cuts...)
- Not well understood since non-perturbative physics is involved.
- Phenomenological models and new tune can be tested looking at the agreement between data and Monte Carlo for various soft QCD distributions.
  - Visible effect in the tuning also at high-p_T (e.g. colour reconnection)

Roberto Di Nardo – University & INFN Tor Vergata

The ATLAS Experiment

The ATLAS Experiment

HADRONIC CALORIMETER:
Iron scintillator Tiles
Resolution $\Delta E/E = 50\%/\sqrt{E(GeV)} \oplus 3\%$

INNER TRACKER:
PIXEL (σ_R=10μm), SCT (σ_R=17μm), TRT (σ_R=50μm), in 2T soleinodal magnetic field

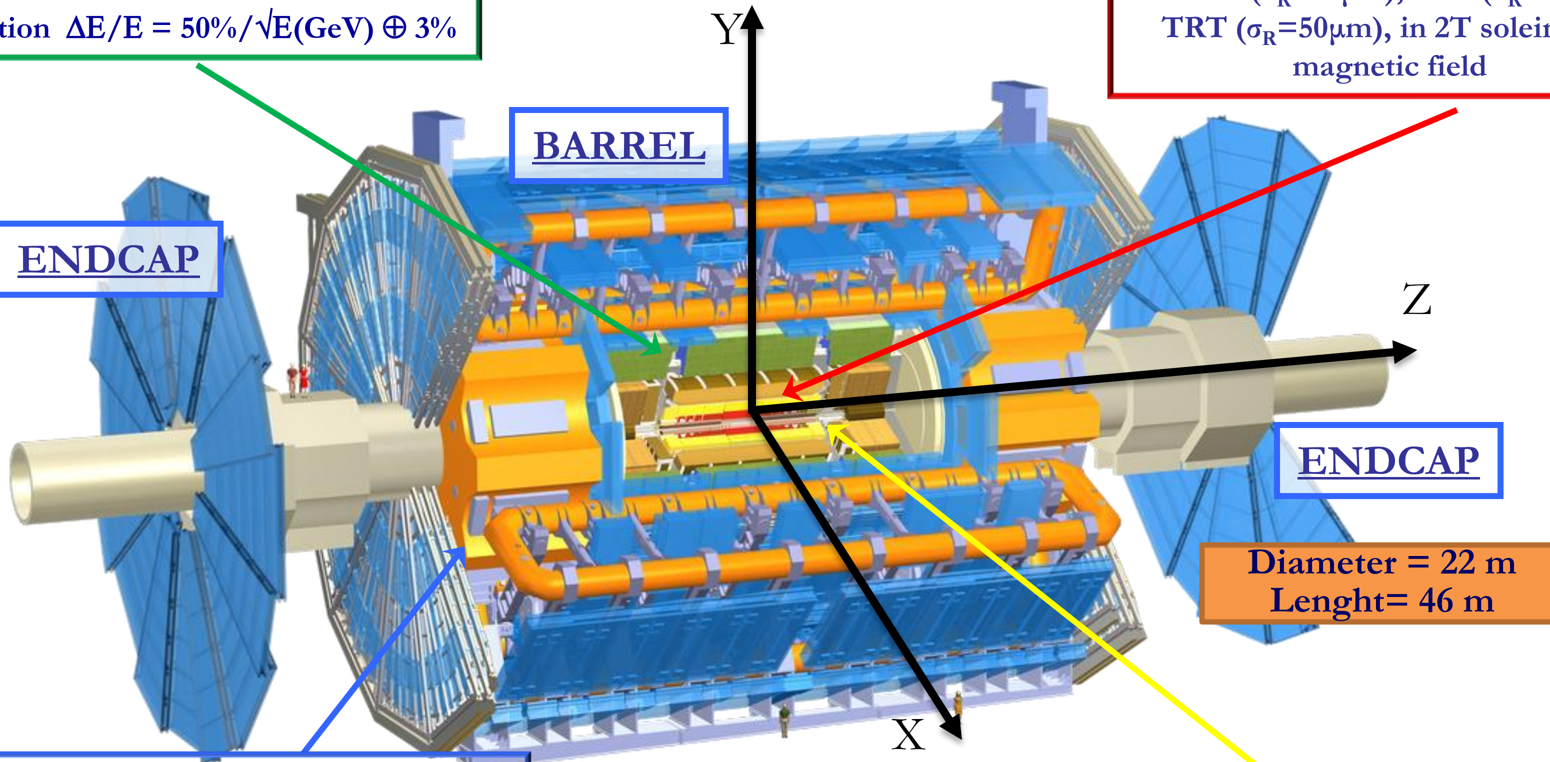

MUON SPECTROMETER:
3 Toroidal magnetic field(1 barrel,2 endcap)
MDT, RPC in the barrel
MDT, TGC , CSC endcap

EM CALORIMETER:
Alternate layers Pb-LAr
Resolution $\Delta E/E = 10\%/\sqrt{E(GeV)} \oplus$
$\oplus 0.5\%/E\ (GeV) \oplus 0.7\%$

Roberto Di Nardo – University & INFN Tor Vergata

The ATLAS Inner Detector

Roberto Di Nardo – University & INFN Tor Vergata

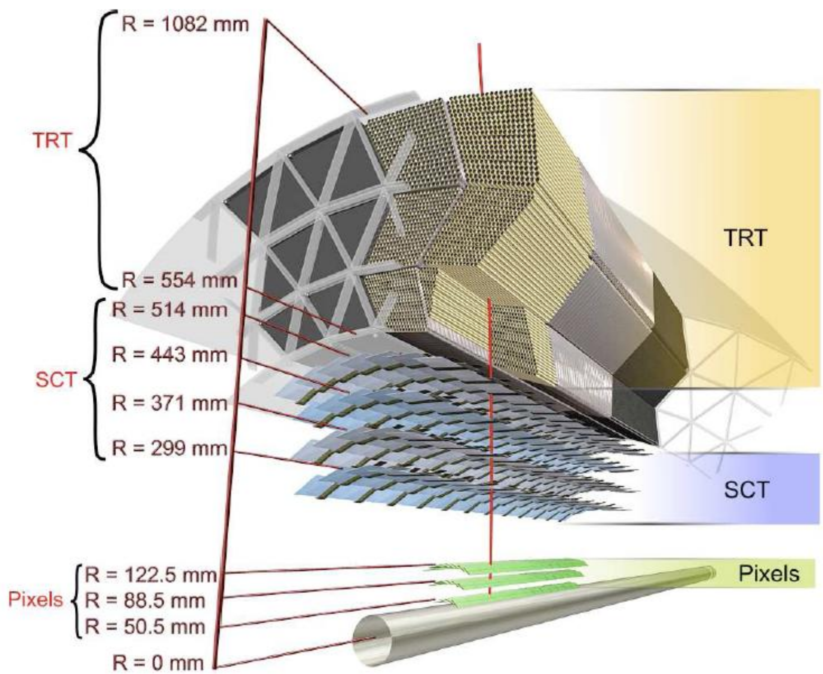

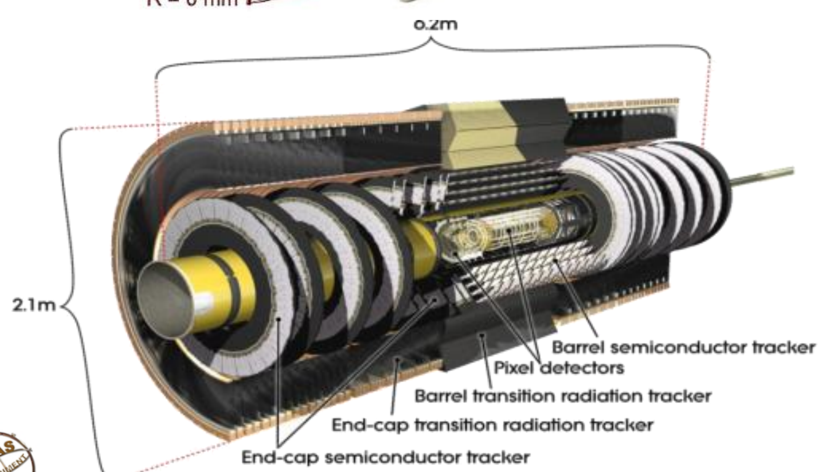

- Covers $|\eta|<2.5$ with 3 subdetectors
- Pixel detector (Silicon Modules)
  - 1774 modules, ~80 M channels
  - Resolutions: ~10 μm (rφ) – ~115 μm (rz)
- SCT detector (Silicon Strip)
  - 4088 modules, ~6.3 M channels
  - Resolutions ~ 17 μm (rφ) – ~580 μm (rz)
- TRT detector (straw drift tubes, $|\eta|<2$)
  - 176 modules, ~0.4 M channels
  - Intrinsic tube resolution ~130 μm (rφ)
  - $e^{+/-}$PID by detection of transition radiation γ

The MBTS trigger

- Minimum Bias Trigger Scintillators used to trigger events to study soft QCD
  - Plastic scintillators
  - Located at 3.56 m from the interaction point on each side
  - Pseudorapidity range covered: $2.09<|\eta|<3.84$
  - Highly efficient for charged particles
  - Different trigger selection possible:
    - 1 hit in either side in coincidence with the BPTX detectors (electrostatic beam pick-up detectors located at 175m from the interaction point)

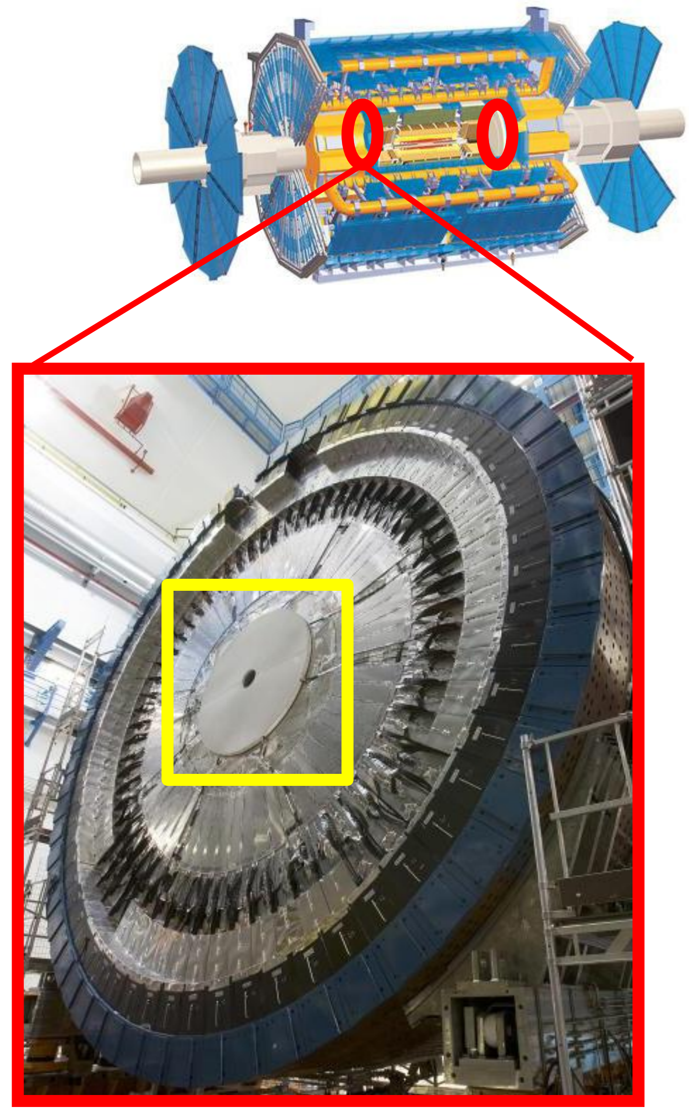

Roberto Di Nardo – University & INFN Tor Vergata

ID performances understanding

Silicon Hit on track

- Good data/MC agreement in the comparison of the average number of silicon hits on track
  - Excellent modelling of the detector in Monte Carlo simualtion

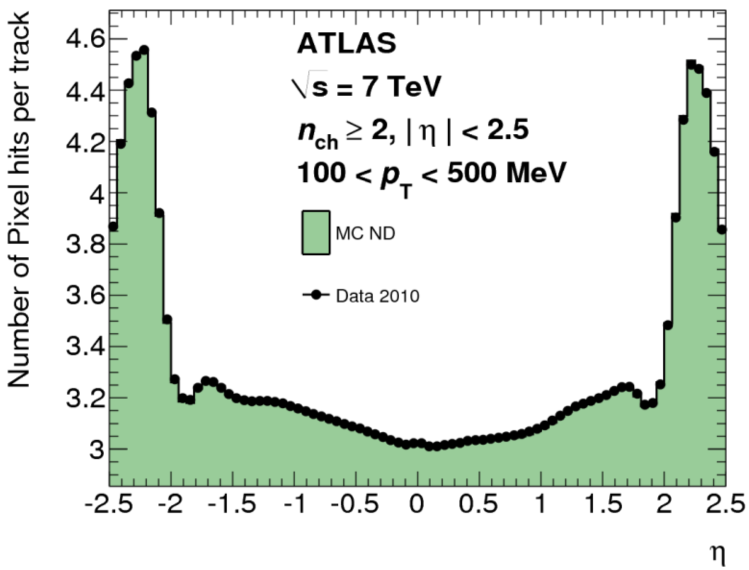

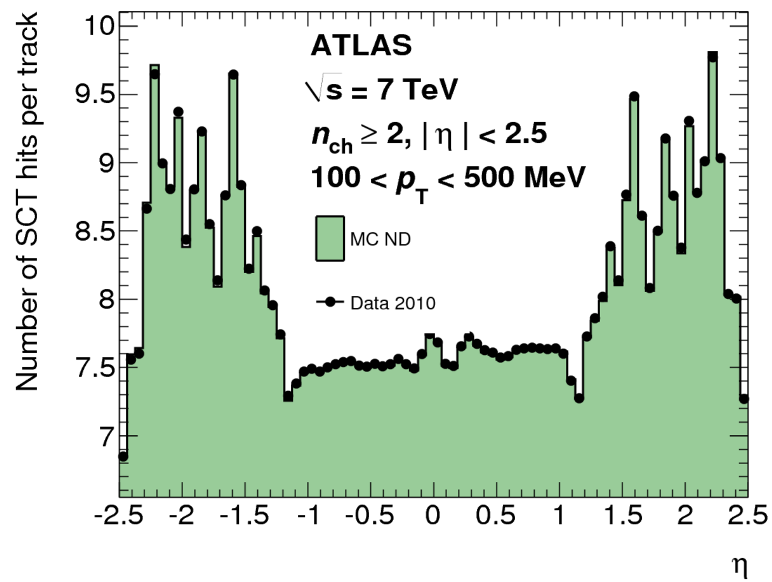

- Uncertainty in the detector material description in simulation→ largest systematic uncertainties in the measurement
  - 10 % material uncertainty reflects into 3% difference in the efficiency

K^0_s and Λ^0 reconstruction

- ~190 μb^{-1} of 7 TeV minimum-bias collision data compared with non-diffractive minimum bias simulation (Pythia ATLAS MC09 tune)
- Pre-selection: tracks with opposite charge, p_T>100MeV , at least 2 silicon hit (Pixel +SCT)

$K^0_s \rightarrow \pi^+\pi^-$ (cτ=2.7cm, BF~69%)

- Transverse Flight Distance > 4 mm
- $\cos(\theta_k)$> 0.999
  - Angle between momentum and flight direction

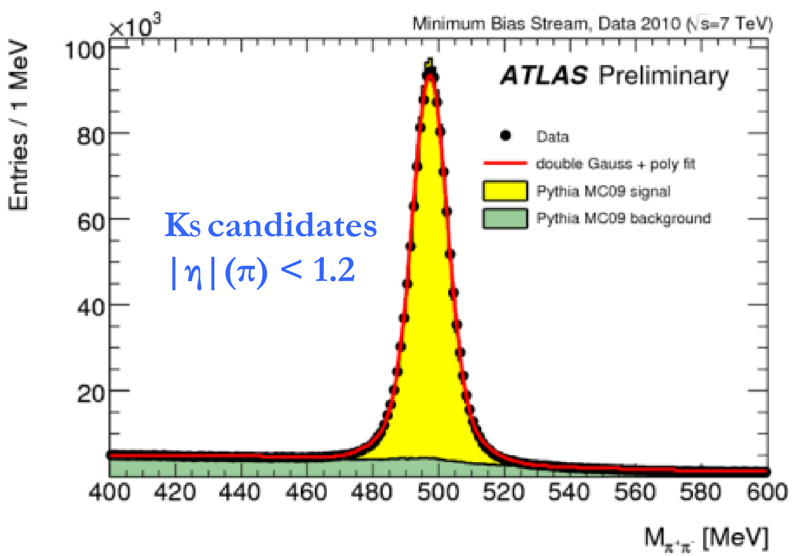

$\Lambda \rightarrow p^+\pi^-$ + c.c.(cτ=7.9cm, BF~64%)

- Flight Distance > 30 mm
- $\cos(\theta_k)$> 0.9998

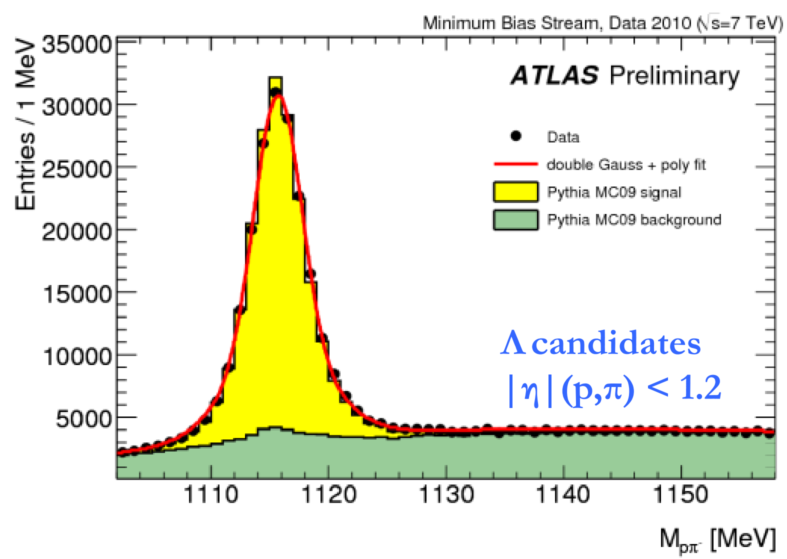

Fitted masses and widths consistent with MC and PDG mass values

Not only K^0_s and Λ

$\Xi^- \rightarrow \Lambda\pi^-$ + c.c. and $\Omega^- \rightarrow \Lambda K^-$ + c.c.

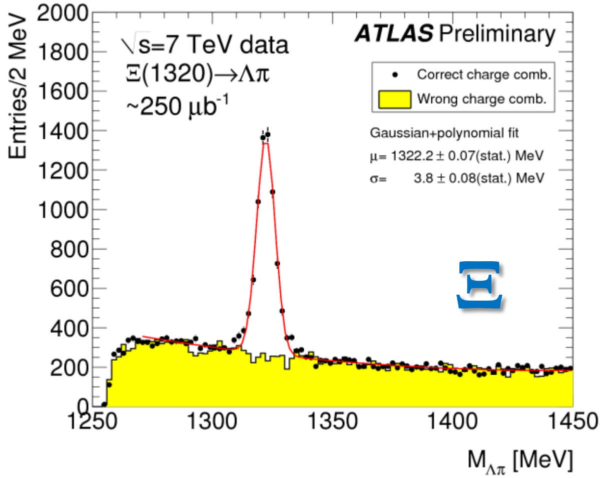

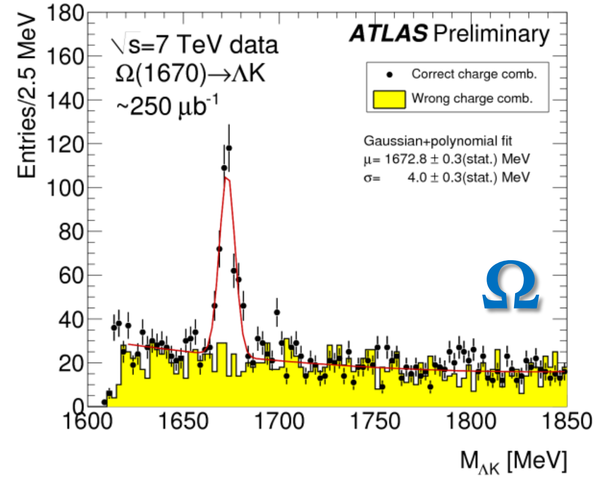

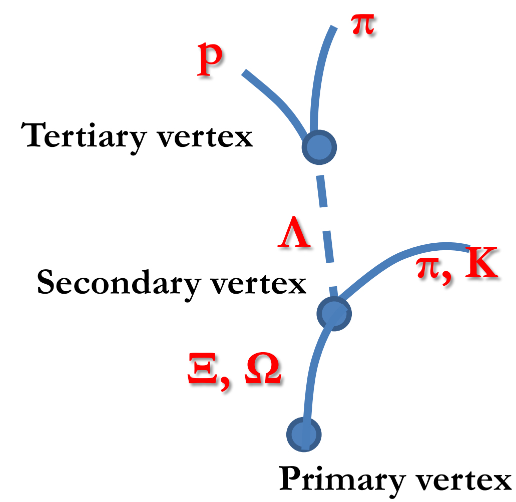

$D^{*+} \rightarrow D^0 (K^-\pi^+)\pi_s^+$ + c.c. and $D_s^+ \rightarrow \Phi(K^+K^-)\,\pi^+$

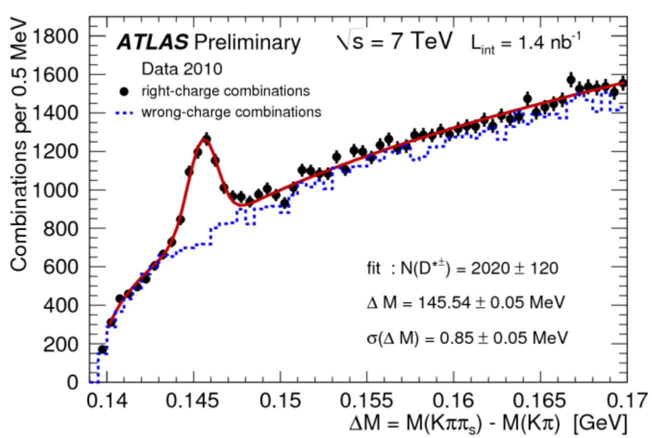

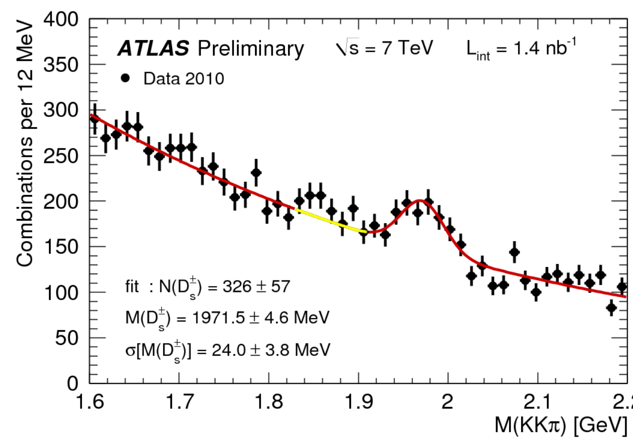

Fitted masses and widths consistent with MC and PDG mass values

Roberto Di Nardo – University & INFN Tor Vergata

Charged particle multiplicity spectra

“Charged particle multiplicities in *pp* interactions measured with the ATLAS detector at the LHC”

- ***arXiv:1012.5104v2 (accepted by New J Phys)***

Dataset and Event Selection

The Datasets:

$\sqrt{s}$=0.9 TeV (~7 μb-1): 360k events; 4.5M tracks

$\sqrt{s}$=7 TeV (~190 μb-1): 10M events; 210M tracks

The Event Selection:

- MBTS single-cell trigger in coincidence with the BPTX (beam pickup)
- 1 Vertex reconstructed
  - 2 tracks + Beam Spot
  - No pileup (secondary vertex with >3 tracks)
- Track quality cuts (hits)
- cut on the impact parameters at the primary vertex to exclude non primary tracks

Phase Space considered : (see arXiv:1012.5104v2 for more than these two)

Most inclusive

- ≥2 good tracks
- p_T > 100 MeV ; $|\eta|$ ≤2.5

Lower diffractive contribution

- ≥6 good tracks
- p_T > 500 MeV ; $|\eta|$ ≤2.5

Roberto Di Nardo – University & INFN Tor Vergata

Correction procedure

- **Event-wise** correction for trigger and vertex efficiencies

$$w_{ev}\left(n_{sel}^{BS}\right)=\frac{1}{\varepsilon_{trig}\left(n_{sel}^{BS}\right)}\cdot\frac{1}{\varepsilon_{vertex}\left(n_{sel}^{BS}\right)}$$

- **Track-wise** correction (e.g. tracking efficiency)

$$w_{ev}(p_T,\eta)=\frac{1}{\varepsilon_{trk}(p_T,\eta)}\cdot(1-f_{Sec}(p_T,\eta))\cdot(1-f_{okr}(p_T,\eta))$$

Fraction of secondaries

Fraction of tracks out of kinematic range

- Takes in to account secondary contamination and tracks out of kinematic range
  - e.g. Track p_T<100 MeV but particle p_T>100 MeV
- N_{ch} and p_T both corrected using a Bayesian unfolding
- $\langle p_T \rangle$ vs n_{ch} → bin-by-bin correction of average p_T and the n_{ch} migration

Efficiencies

- **Trigger** and **Vertex** efficiencies both measured from data

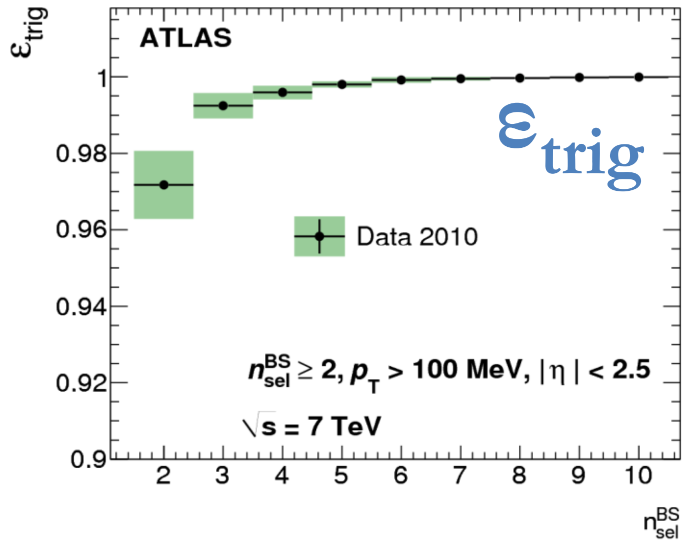

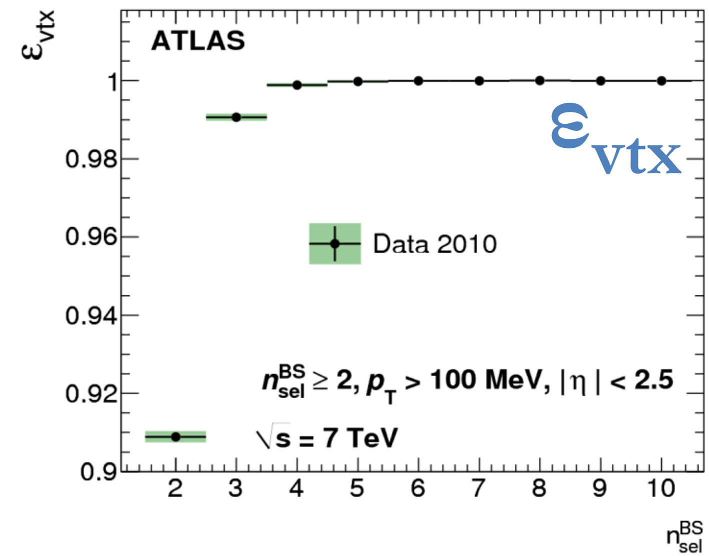

- **Tracking** efficiencies evaluated in MC simulation

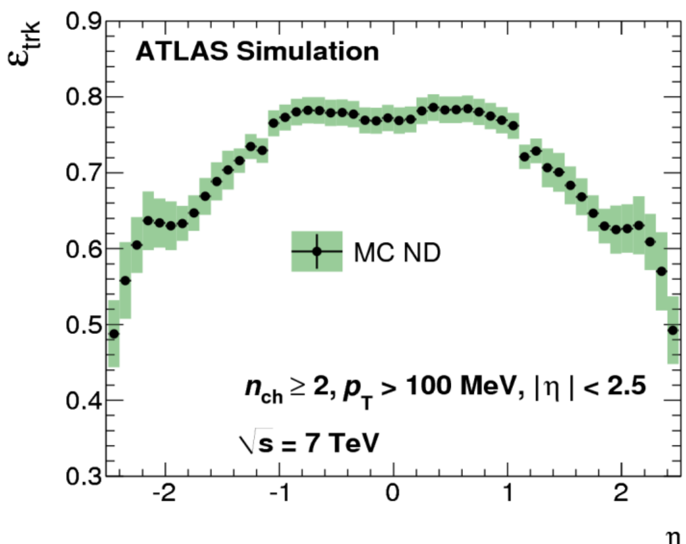

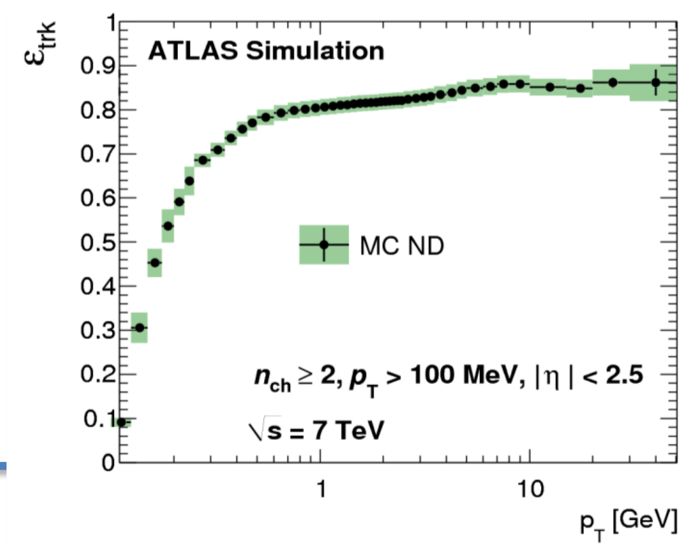

$1/N_{ev} dN_{ch}/d\eta$

- **Different models differ in normalization but the shape are almost similar**
  - **Phojet gives the best description of 900 GeV data**
  - **At 7 TeV Track multiplicity underestimated for all the models.**
  - **The variation of the shape between models is little**
- **$n_{ch}\geq6$, p_T>500MeV measurement used in AMBT1 tune**

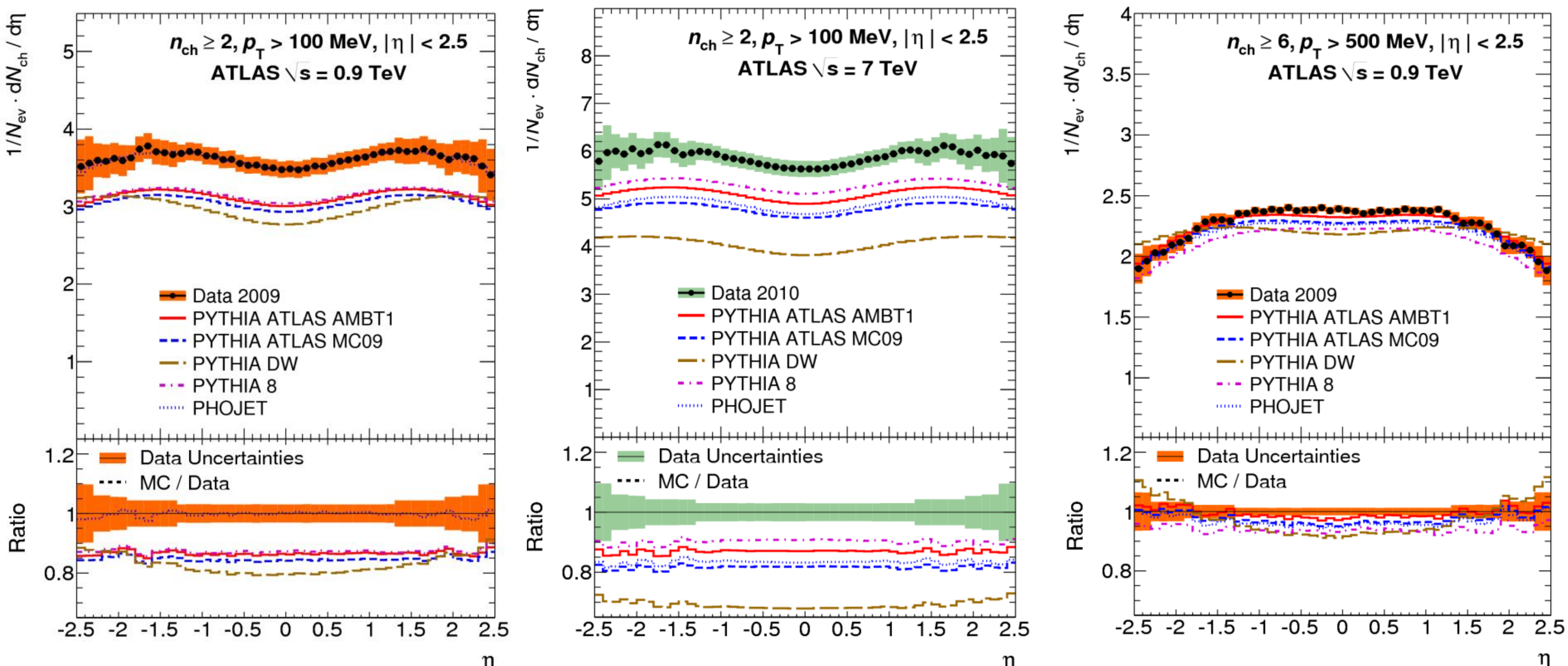

$n_{ch}\geq2$, p_T>100MeV

$n_{ch}\geq6$, p_T>500MeV

$1/(2\pi p_T) 1/N_{ev} d^2N_{ch}/d\eta dp_T$

- Measurement spans 10 orders of magnitude
- Large disagreement at low p_T and high p_T
  - better agreement in the range 0.5-3 GeV
- AMBT1 have a better agreement in the medium p_T region

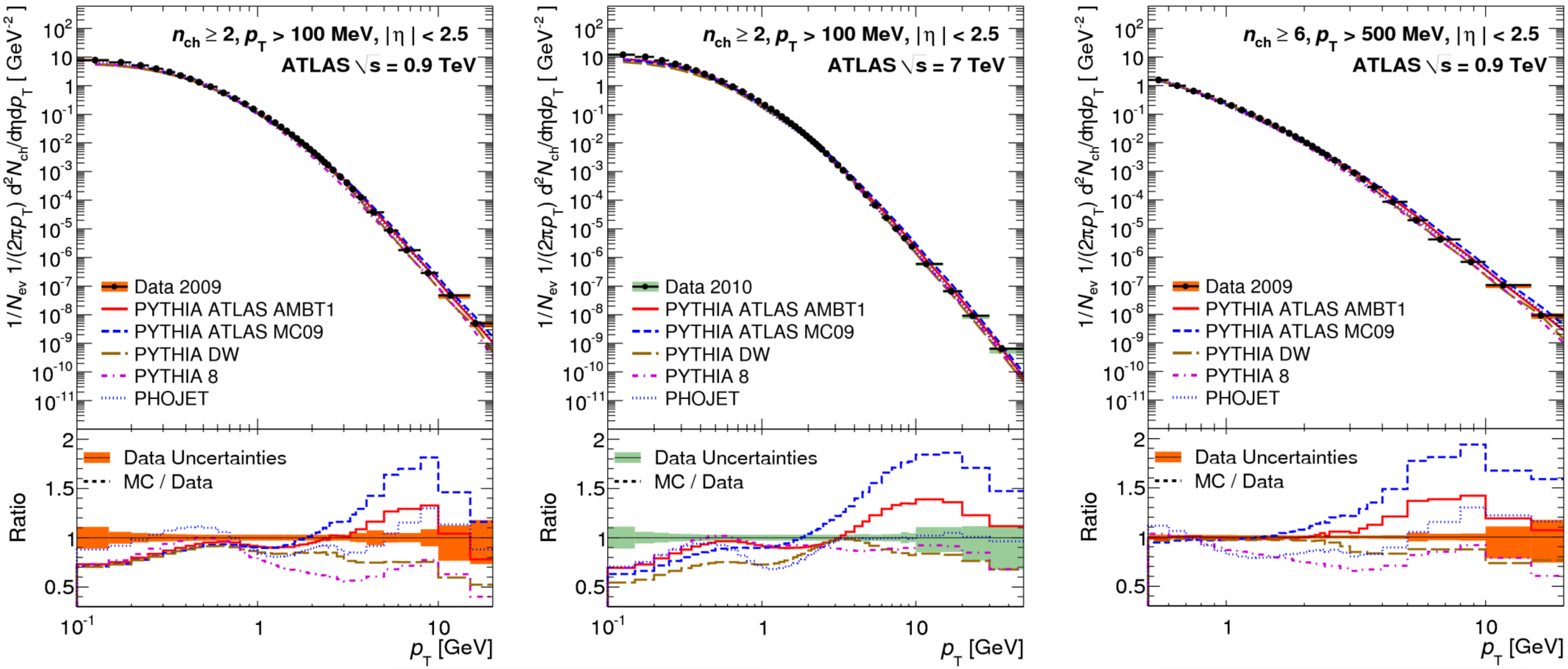

$n_{ch} \geq 2$, p_T>100MeV

$n_{ch} \geq 6$, p_T>500MeV

$1/N_{ev} dN_{ev}/dN_{ch}$

- The low n_{ch} region not well modeled by any MC
  - large contribution from diffractive component
- The peak at 10 particles well described by the new AMBT1 tune

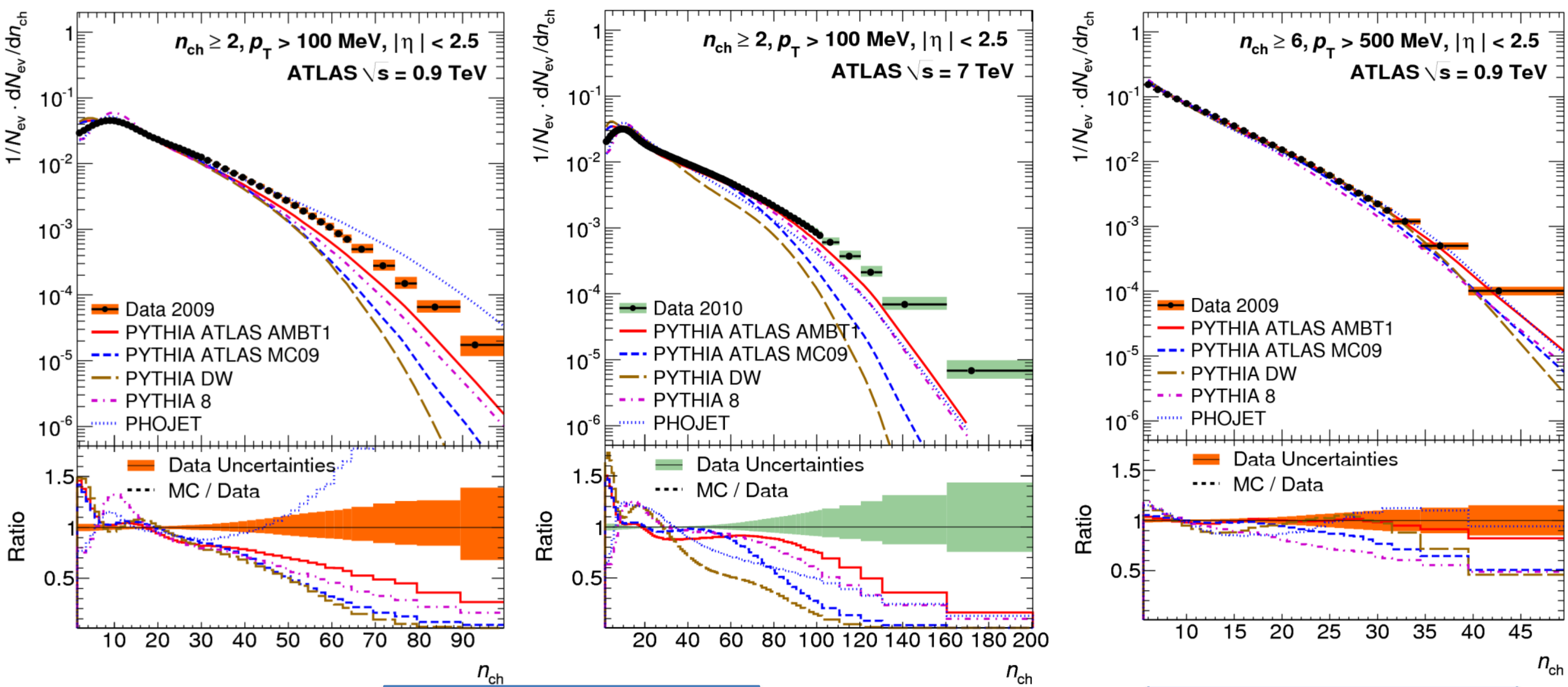

$n_{ch} \geq 2$, $p_T > 100$MeV

$n_{ch} \geq 6$, $p_T > 500$MeV

$< p_T >$ vs N_{ch}

- Predictions differ significantly between the different models in particular at high n_{ch}
- Best description from AMBT1 and Pythia8
  - Shape at high p_T well modelled
- High sensitivity of the low n_{ch} shape linked to the different ND,SD,DD fractions

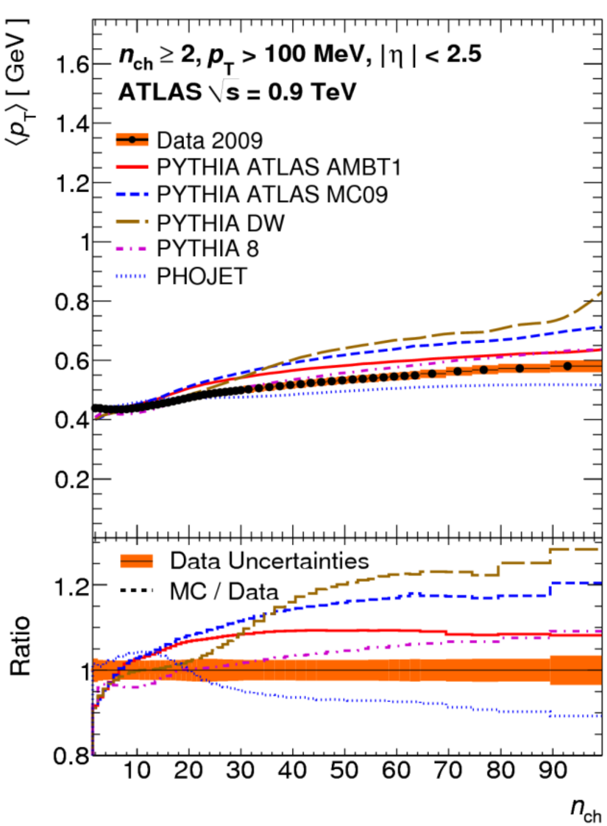

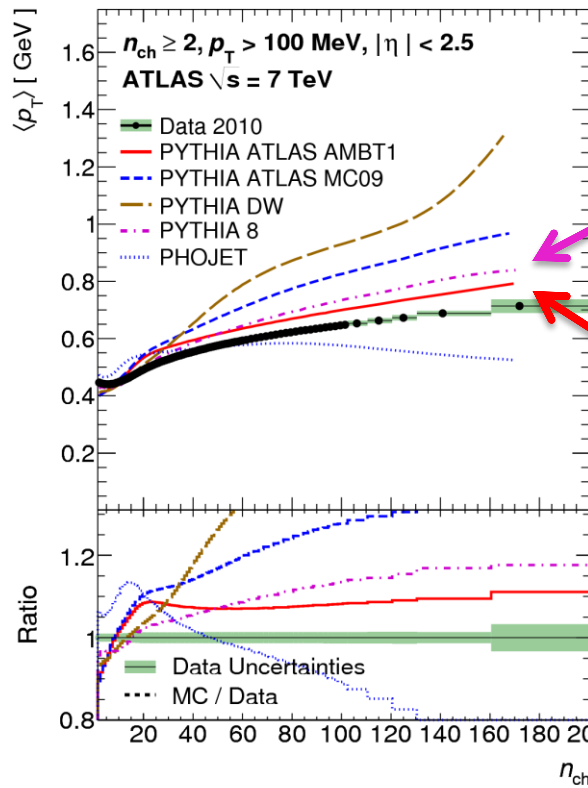

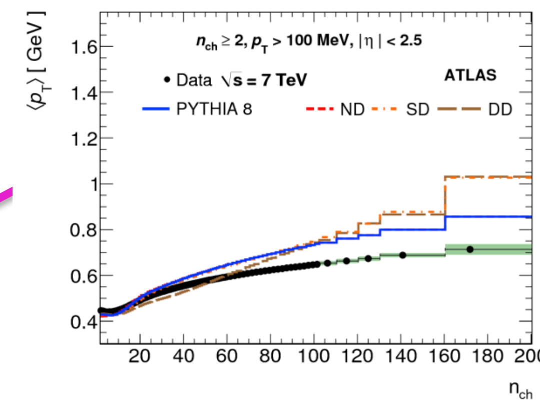

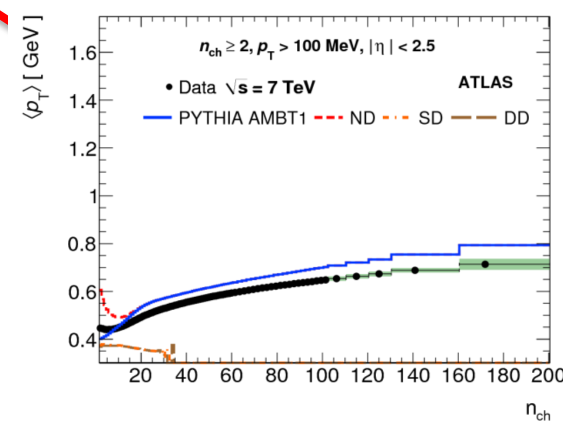

$n_{ch} \geq 2$, p_T>100MeV

Roberto Di Nardo – University & INFN Tor Vergata

Underlying Events

- **"Measurement of underlying event characteristics using charged particles in pp collisions at √s = 900 GeV and 7 TeV with the ATLAS detector"**
    - ***arXiv:1012.0791v2 (accepted by Phys Rev D)***

- **"Measurements of underlying event properties using neutral and charged particles in p-p collisions at 900 GeV and 7 TeV with the ATLAS detector at the LHC"**
    - ***arXiv:1103.1816v2 (submitted to EPJC)***

Underlying Events

- "Underlying Event": everything except the hard scattering process
  - MPI, ISR-FSR contributions, beam-beam remnants
- Transverse region: perpendicular to the hard scattering and sensitive to the underlying event
  - Used the leading track to identify the leading jet - 60°<|Δφ|<120°

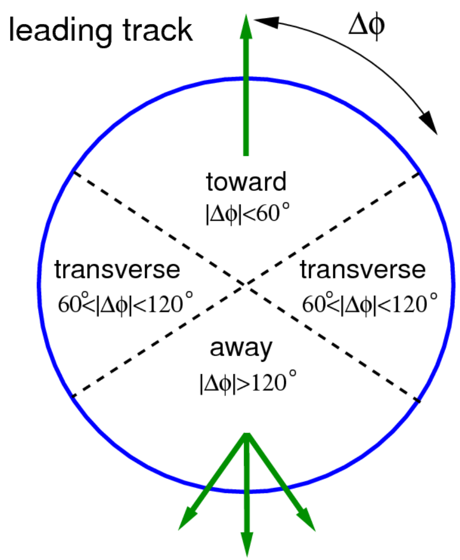

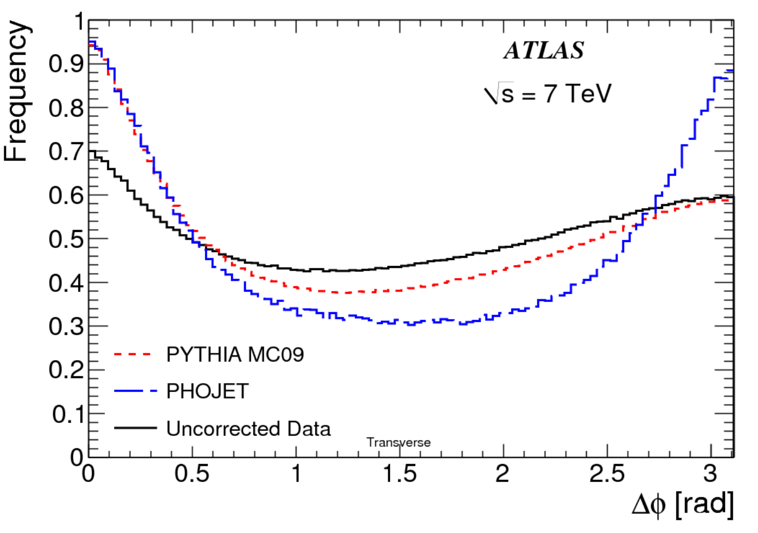

- same correction for trigger, vertex and tracking efficiency as in the Charged Multiplicities distribution analysis

Angular distributions vs p_T^{lead}

- Charged particle number density for tracks other than the leading track
  - plot reflected wrt $\Delta\varphi=0$
  - Jet-like shape (higher tracks population in the toward and the away region) is most evident for harder leading tracks

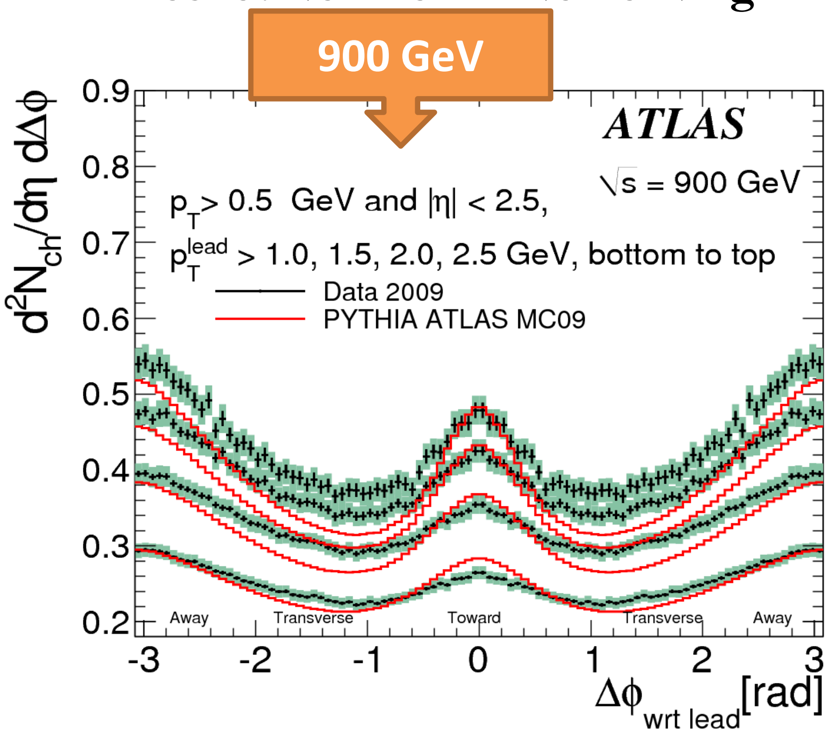

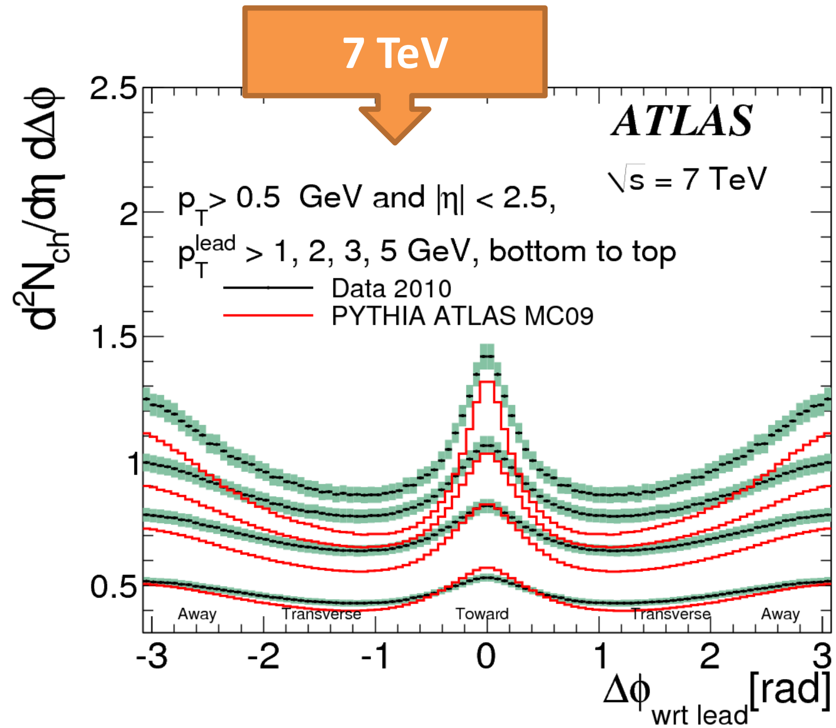

- different densities and different angular distributions between data and MC

Multiplicity

- Density of charged particle (p_T>500MeV $|\eta|$<2.5) as function of the leading track p_T in the transverse region increase of a factor 2 form 900 GeV to 7 TeV .

900 GeV

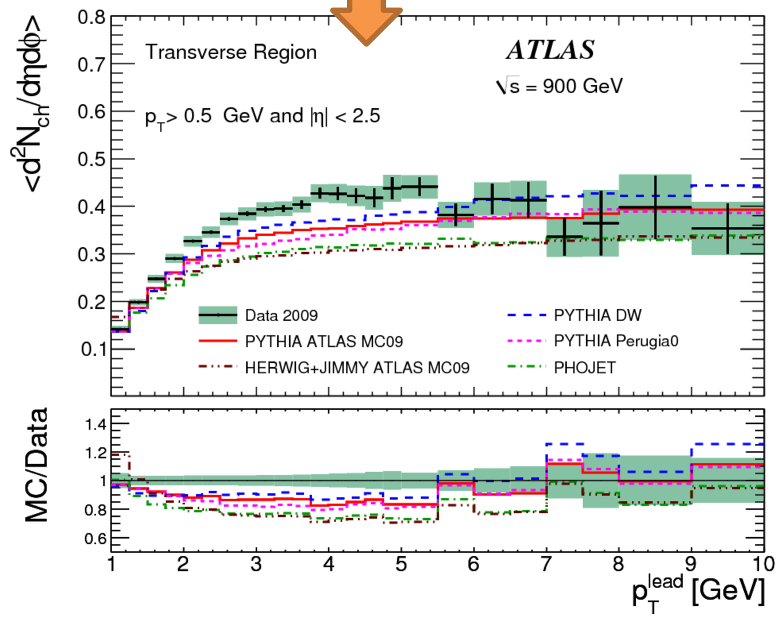

7 TeV

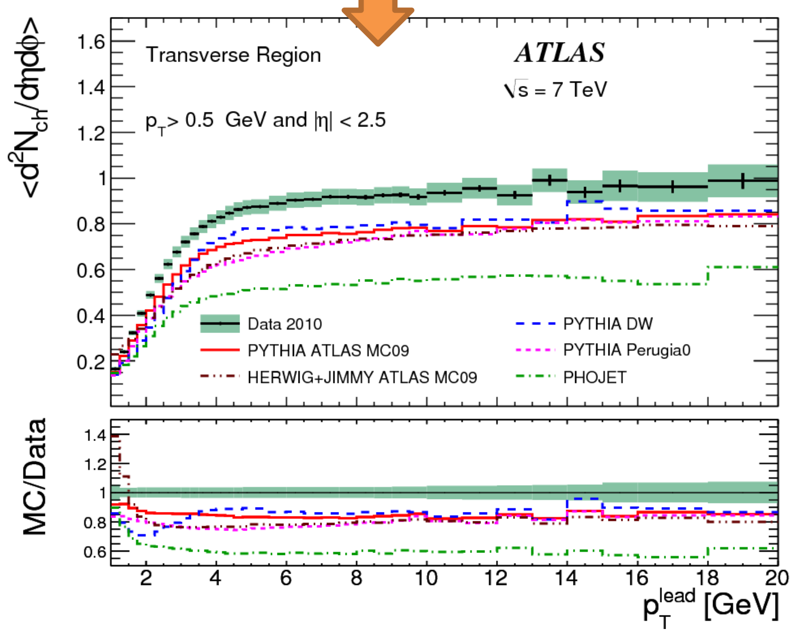

- Plateau value is a factor 2 larger as seen in the Minimum Bias events (due to the high p_T track selection effect: more momentum exchange and lack of diffractive contributions in events with p_T^{lead} in plateau region)

Scalar Σp_T density

Roberto Di Nardo – University & INFN Tor Vergata

900 GeV

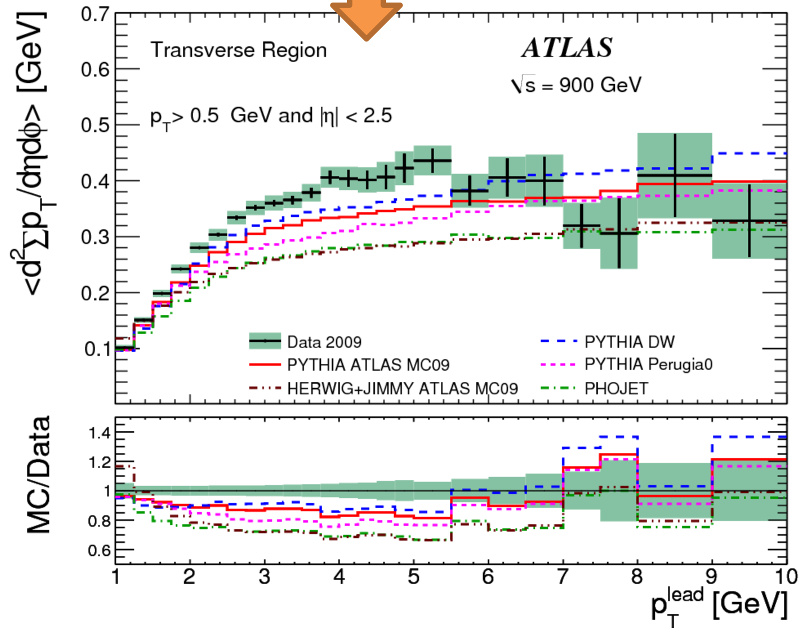

7 TeV

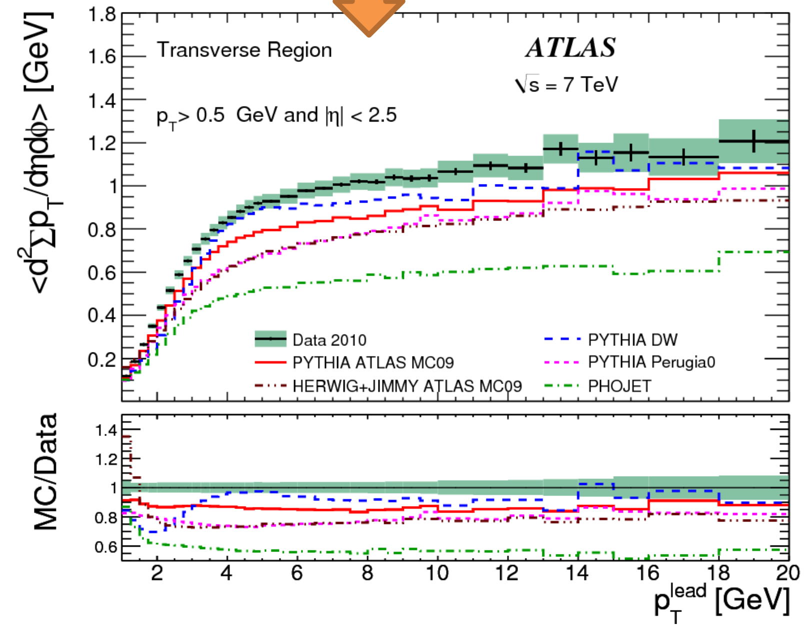

- **None of the tune describe the data well**
  - **DW is the closest to data**
  - **Other tunes underestimate the density.**

Lower p_T threshold

900 GeV

7 TeV

multiplicity

Scalar Σp_T density

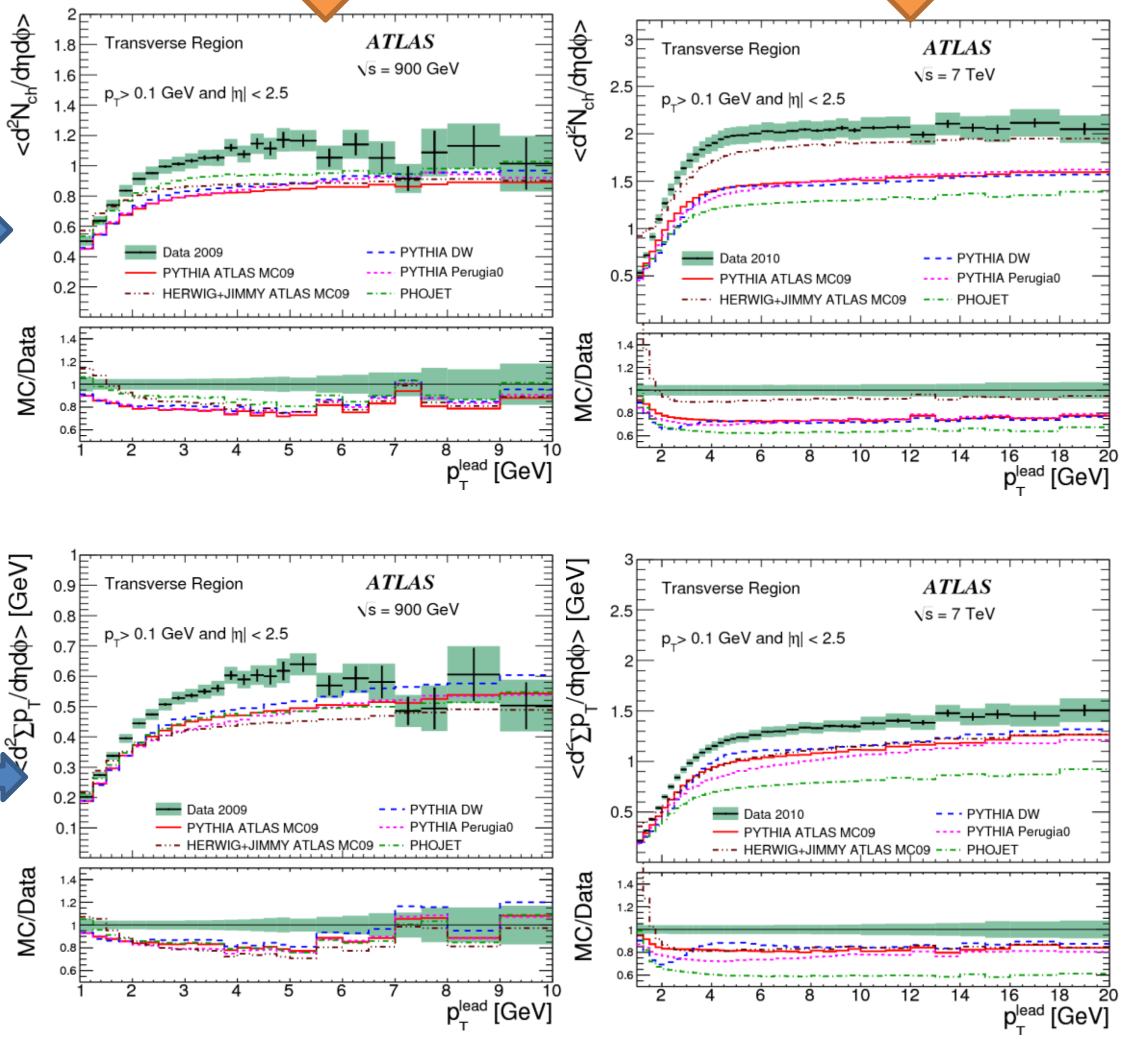

- ➢ UE measurements performed also with a lower p_T threshold
- ➢ $p_T > 100$ MeV, $|\eta| < 2.5$
- ➢ Poorly reproduced by models which have a better agreement for $p_T > 500$ MeV

Roberto Di Nardo – University & INFN Tor Vergata

UE with charged and neutral particles

- Calorimeter based UE measurements
  - Sensitive to the neutral component → integrate the result of the track based analysis

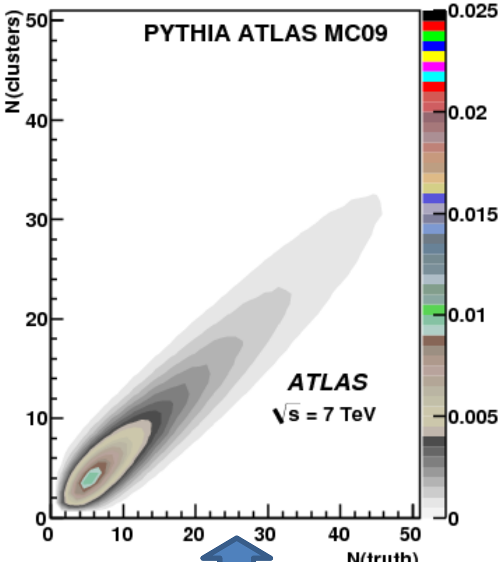

Topocluster vs truth particles (MC)

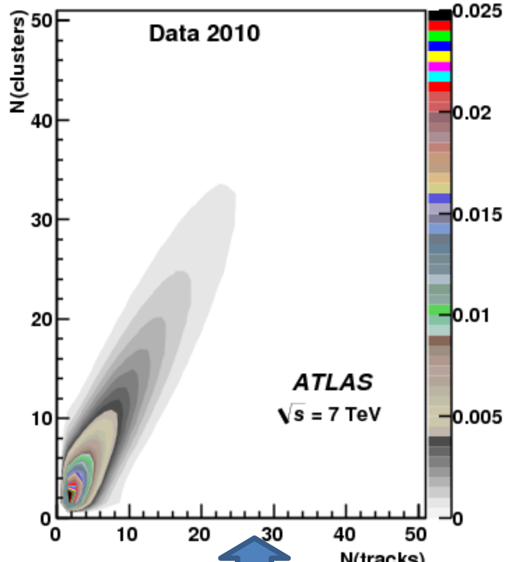

Topocluster vs reco tracks (data)

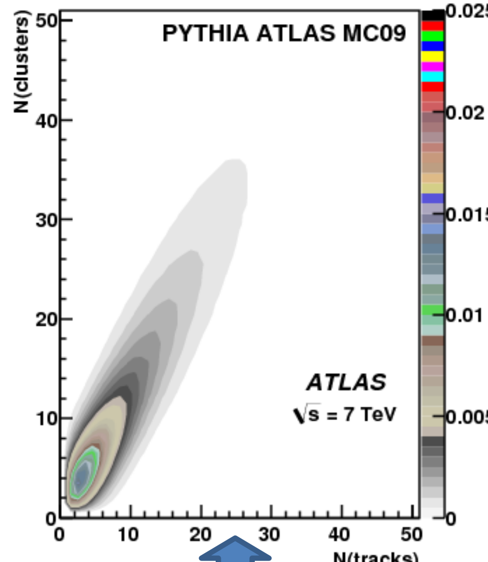

Topocluster vs reco tracks (MC)

- High calorimetric segmentation:
  - EM $\Delta\eta \times \Delta\varphi$: 0.003 × 0.1 – 0.05 × 0.025
  - HAD $\Delta\eta \times \Delta\varphi$: 0.1 × 0.1
- TopoCluster selection :
  - p_T>500 MeV
  - $|\eta|$<2.5

Angular distributions

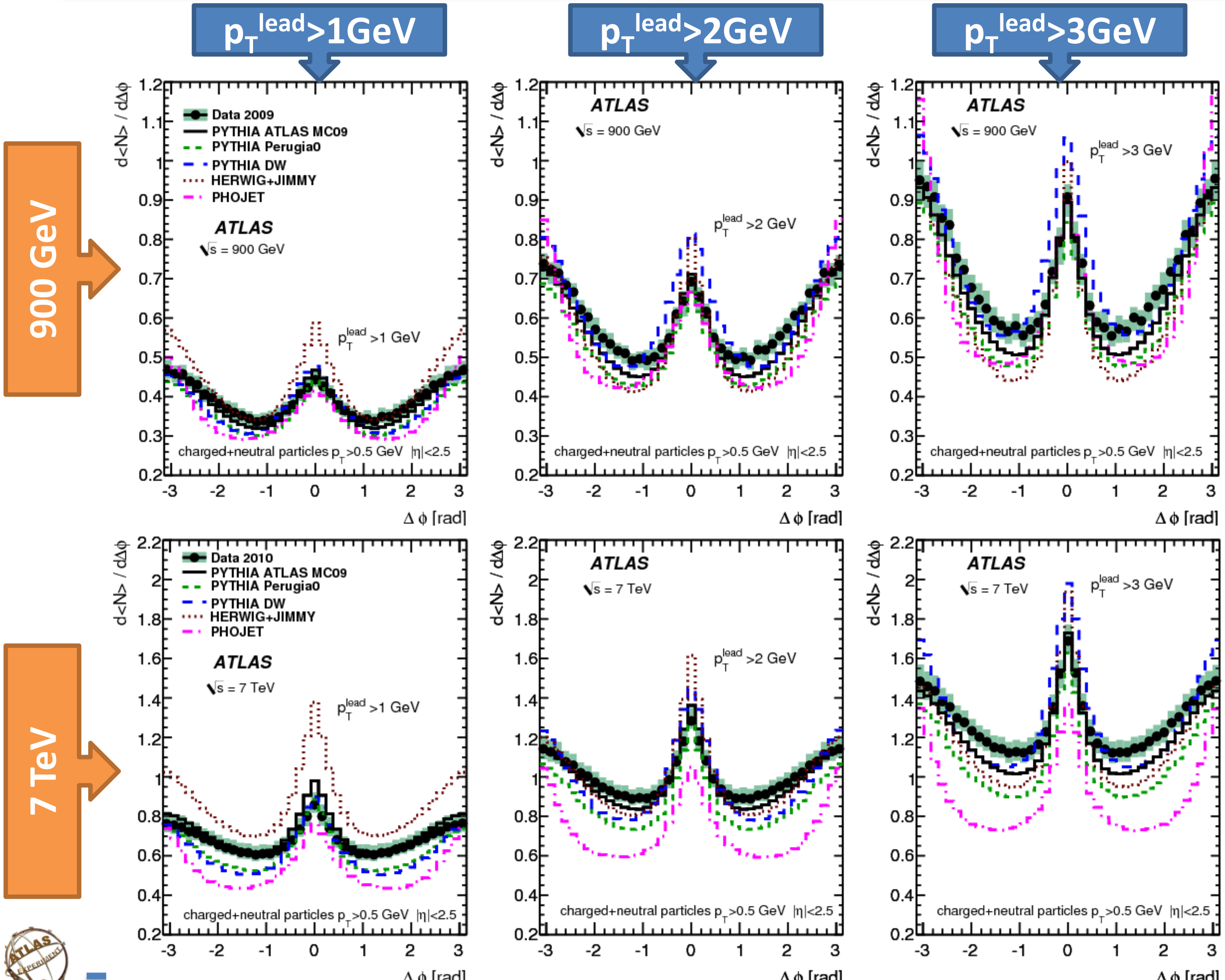

- ➢Densities are 40% higher with respect to the UE with only charged tracks due to the neutral component
- ➢None of the MC describes properly the data
- ➢Pythia DW and Herwig overestimate data for $\Delta\varphi \sim 0$
- ➢Phojet underestimate data

Multiplicity

- Particle multiplicities in the transverse region
- Lower particles densities for the various MC tunes wrt data
  - PYTHIA DW is the closest to the data
  - PHOJET underestimate the multiplicities

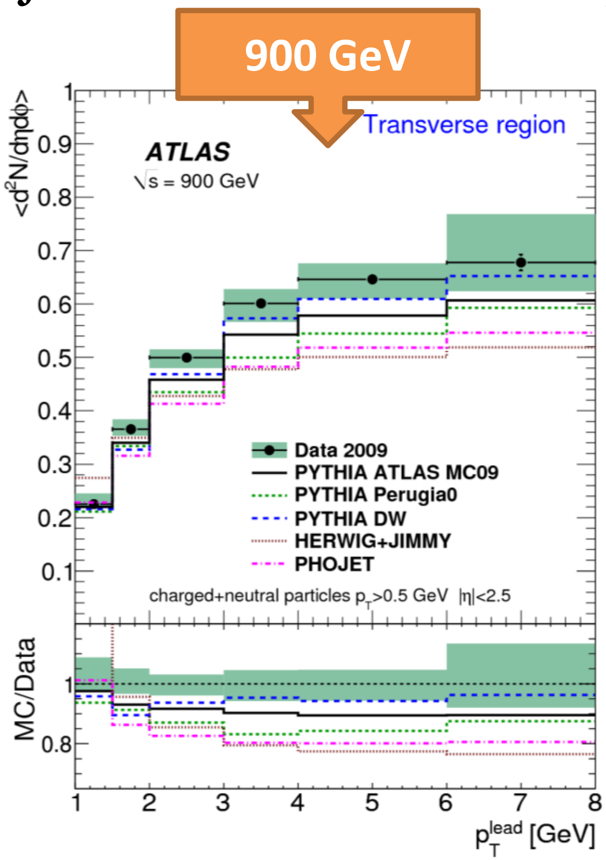

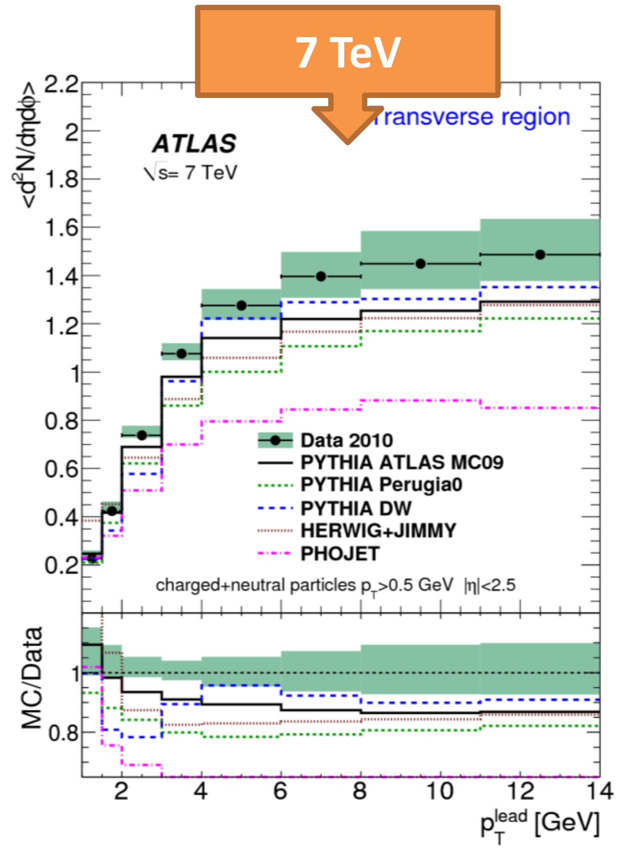

Two-particle angular correlation

Roberto Di Nardo – University & INFN Tor Vergata

Two-particle angular correlations

- The study of correlations between final state particles is a powerful method for investigating the underlying mechanisms of particle production

- The correlation function is given by:

Correlation between emission in a single event

$$R(\Delta\eta, \Delta\phi) = \frac{\langle (N_{ch} - 1)\, F(N_{ch}, \Delta\eta, \Delta\phi) \rangle_{ch}}{B(\Delta\eta, \Delta\phi)} - \langle N_{ch} - 1 \rangle_{ch}$$

Distribution of uncorrelated pairs

- Different region can be distinguished for the correlation function in $\Delta\eta\Delta\varphi$ plane
  - $\Delta\varphi \sim \pi \rightarrow$ back to back jets (away side correlations)
  - $\Delta\varphi \sim 0 \rightarrow$ particles in a single jet (near side correlations)
  - $|\Delta\eta| < 2 \rightarrow$ resonances, string fragmentation, clusters (short range correlations)

Two-particle angular correlations

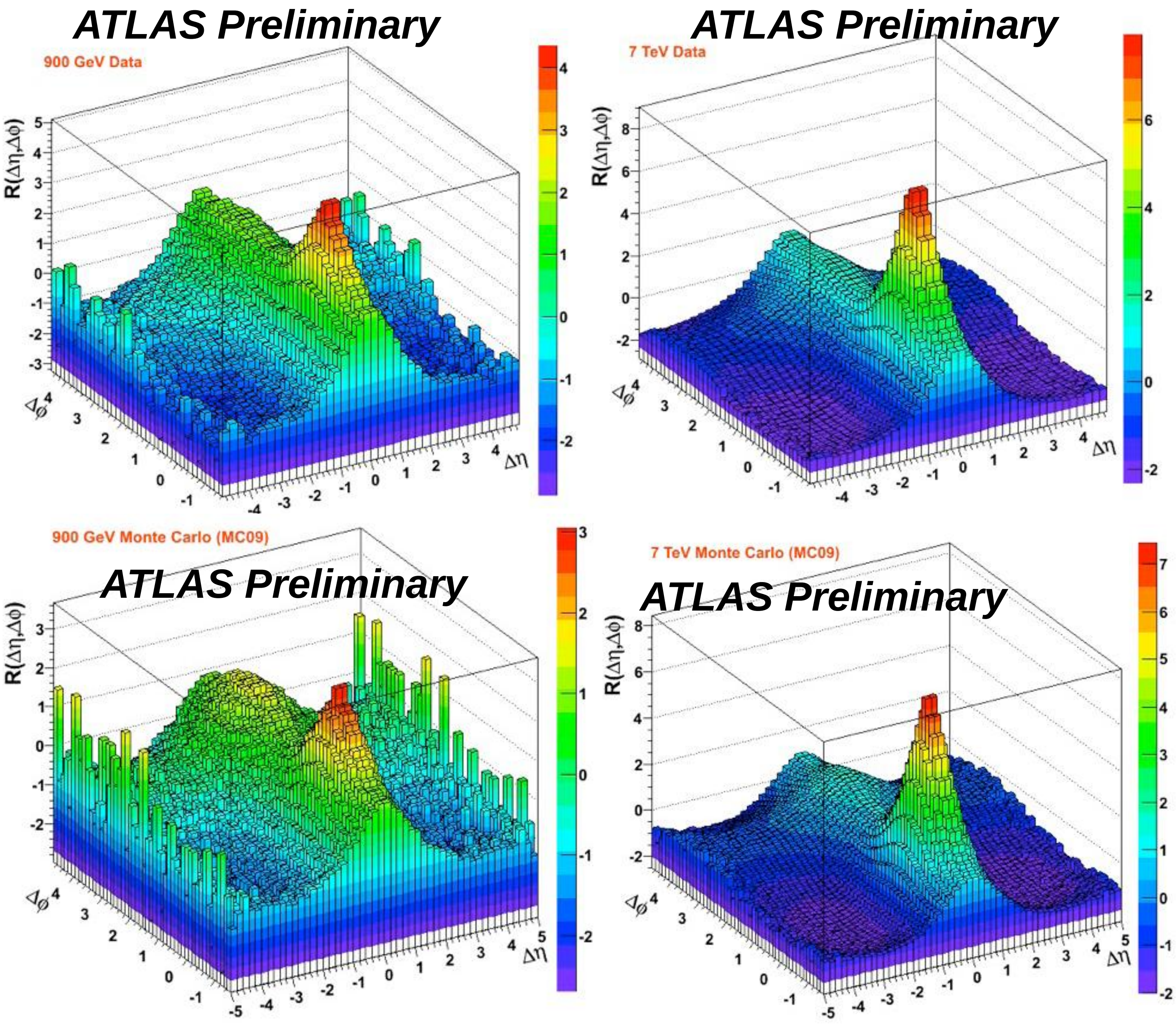

- After correction procedure
- The correlation function in Pythia tune MC09 shows similar structure
- Strength of the correlation different between data and MC

R(Δη,Δφ) projections

Away-side | **near-side** | **Short range**

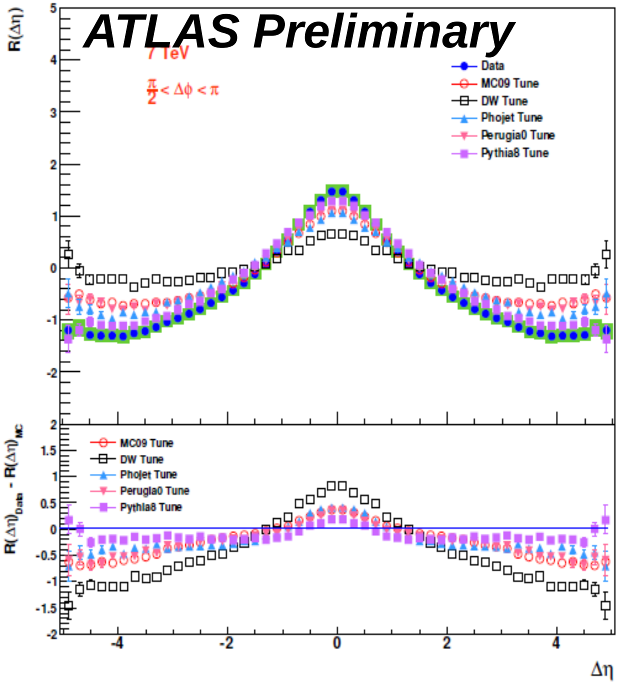

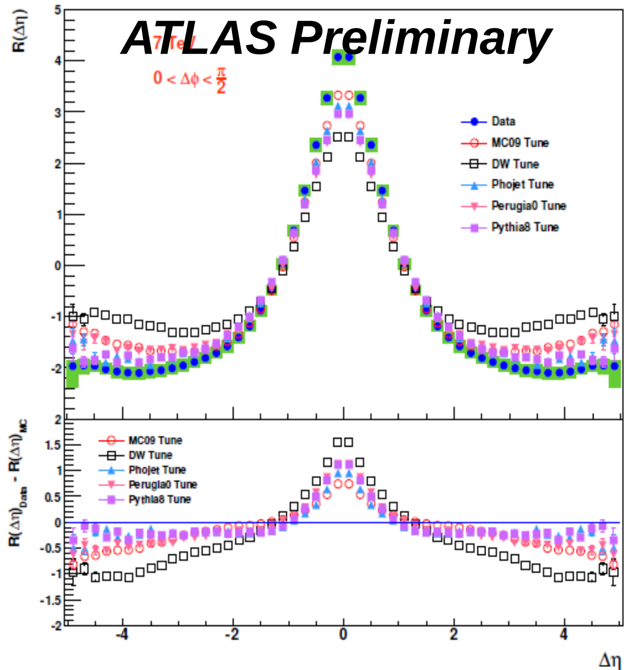

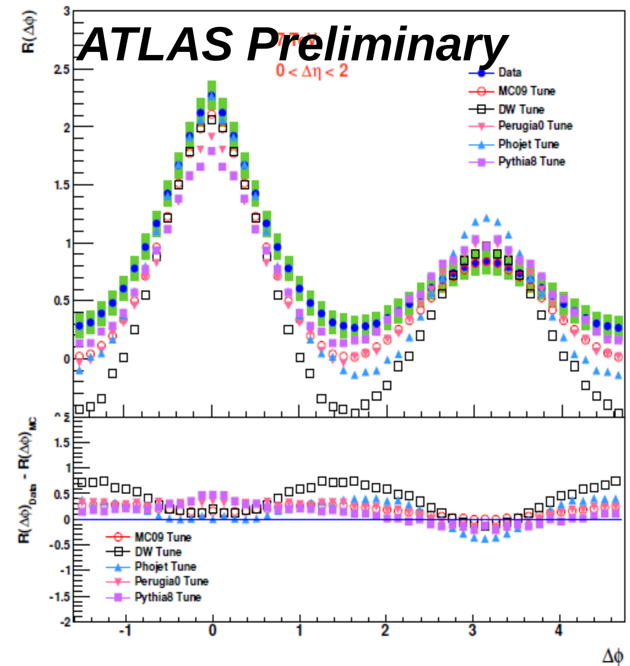

- **Away-side: good agreement between data and Pythia8 in the full range**
- **Near-side: none of the tunes have the right shape. Pythia8 closest to data in the tails**
- **Short-range: different tunes agree with data only in localized regions**

Conclusions

- Performances of the ATLAS Inner Detector well understood
  - Reconstruction of numerous resonances demonstrates accurate momentum scale and modeling of tracking in the multiple-scattering regime
- Minimum bias data taken by the ATLAS detector for $\sqrt{s}$ = 0.9, 2.36, 7 TeV have been analyzed
  - good description of data for p_T>500 MeV with the AMBT1, worst agreement for a lower p_T threshold (p_T>100 MeV)
- Results for Underlying Events in pp collisions at $\sqrt{s}$ = 900 GeV and $\sqrt{s}$ = 7 TeV at ATLAS have been presented
- Two-particle angular correlation function has been measured at 900 GeV and 7 TeV.
  - None of the MC models reproduce the strength of the correlation (Pythia8 closest to the data)

Backup

Tunings

- The basic components of Pythia that require tuning are the descriptions of:
  - Final state radiation and hadronisation,
  - Initial state radiation and primordial kT ,
  - Underlying event, beam remnants, colour reconnection, and
  - Energy scaling.

- Perugia0
  - PYTHIA Tune based on Minimum bias results from CDF and UA5. No UE data used
  - CTEQ5L parton distribution functions used
- DW
  - PYTHIA Tune that use CDF UE and Drell-Yan data (no Min Bias Data)
- ATLAS MC09
  - PYTHIA Tune based on CDF Minnimum Bias and UE Measurements (RUN I and II) plus the D0 results on dijet angular correlations

Roberto Di Nardo – University & INFN Tor Vergata

ATLAS data in AMBT1

Analysis	Observable	Tuning range
ATLAS 0.9 TeV, minimum bias, $n_{ch} \geq 6$	$\frac{1}{N_{ev}} \cdot \frac{dN_{ch}}{d\eta}$	-2.5 – 2.5
ATLAS 0.9 TeV, minimum bias, $n_{ch} \geq 6$	$\frac{1}{N_{ev}} \cdot \frac{1}{2\pi p_T} \cdot \frac{d^2 N_{ch}}{d\eta d p_T}$	≥ 5.0
ATLAS 0.9 TeV, minimum bias, $n_{ch} \geq 6$	$\frac{1}{N_{ev}} \cdot \frac{dN_{ev}}{dn_{ch}}$	≥ 20
ATLAS 0.9 TeV, minimum bias, $n_{ch} \geq 6$	$\langle p_T \rangle$ vs. n_{ch}	≥ 10
ATLAS 0.9 TeV, UE in minimum bias	$\langle \frac{d^2 N_{chg}}{d\eta d\phi} \rangle$ (towards)	≥ 5.5 GeV
ATLAS 0.9 TeV, UE in minimum bias	$\langle \frac{d^2 N_{chg}}{d\eta d\phi} \rangle$ (transverse)	≥ 5.5 GeV
ATLAS 0.9 TeV, UE in minimum bias	$\langle \frac{d^2 N_{chg}}{d\eta d\phi} \rangle$ (away)	≥ 5.5 GeV
ATLAS 0.9 TeV, UE in minimum bias	$\langle \frac{d^2 \sum p_T}{d\eta d\phi} \rangle$ (towards)	≥ 5.5 GeV
ATLAS 0.9 TeV, UE in minimum bias	$\langle \frac{d^2 \sum p_T}{d\eta d\phi} \rangle$ (transverse)	≥ 5.5 GeV
ATLAS 0.9 TeV, UE in minimum bias	$\langle \frac{d^2 \sum p_T}{d\eta d\phi} \rangle$ (away)	≥ 5.5 GeV
ATLAS 7 TeV, minimum bias, $n_{ch} \geq 6$	$\frac{1}{N_{ev}} \cdot \frac{dN_{ch}}{d\eta}$	-2.5 – 2.5
ATLAS 7 TeV, minimum bias, $n_{ch} \geq 6$	$\frac{1}{N_{ev}} \cdot \frac{1}{2\pi p_T} \cdot \frac{d^2 N_{ch}}{d\eta d p_T}$	≥ 5.0
ATLAS 7 TeV, minimum bias, $n_{ch} \geq 6$	$\frac{1}{N_{ev}} \cdot \frac{dN_{ev}}{dn_{ch}}$	≥ 40
ATLAS 7 TeV, minimum bias, $n_{ch} \geq 6$	$\langle p_T \rangle$ vs. n_{ch}	≥ 10
ATLAS 7 TeV, UE in minimum bias	$\langle \frac{d^2 N_{chg}}{d\eta d\phi} \rangle$ (towards)	≥ 10 GeV
ATLAS 7 TeV, UE in minimum bias	$\langle \frac{d^2 N_{chg}}{d\eta d\phi} \rangle$ (transverse)	≥ 10 GeV
ATLAS 7 TeV, UE in minimum bias	$\langle \frac{d^2 N_{chg}}{d\eta d\phi} \rangle$ (away)	≥ 10 GeV
ATLAS 7 TeV, UE in minimum bias	$\langle \frac{d^2 \sum p_T}{d\eta d\phi} \rangle$ (towards)	≥ 10 GeV
ATLAS 7 TeV, UE in minimum bias	$\langle \frac{d^2 \sum p_T}{d\eta d\phi} \rangle$ (transverse)	≥ 10 GeV
ATLAS 7 TeV, UE in minimum bias	$\langle \frac{d^2 \sum p_T}{d\eta d\phi} \rangle$ (away)	≥ 10 GeV

Tevatron data in AMBT1

CDF Run I underlying event in dijet events[13] (leading jet analysis)
N_{ch} density vs leading jet p_T (transverse), JET20
N_{ch} density vs leading jet p_T (toward), JET20
N_{ch} density vs leading jet p_T (away), JET20
$\sum p_T$ density vs leading jet p_T (transverse), JET20
$\sum p_T$ density vs leading jet p_T (toward), JET20
$\sum p_T$ density vs leading jet p_T (away), JET20
N_{ch} density vs leading jet p_T (transverse), min bias
N_{ch} density vs leading jet p_T (toward), min bias
N_{ch} density vs leading jet p_T (away), min bias
$\sum p_T$ density vs leading jet p_T (transverse), min bias
$\sum p_T$ density vs leading jet p_T (toward), min bias
$\sum p_T$ density vs leading jet p_T (away), min bias
p_T distribution (transverse), leading $p_T > 5$ GeV
p_T distribution (transverse), leading $p_T > 30$ GeV
CDF Run I underlying event in MIN/MAX-cones[14] ("MIN-MAX" analysis)
$\langle p_T^{max} \rangle$ vs. E_T^{lead}, $\sqrt{s} = 1800$ GeV
$\langle p_T^{min} \rangle$ vs. E_T^{lead}, $\sqrt{s} = 1800$ GeV
$\langle p_T^{diff} \rangle$ vs. E_T^{lead}, $\sqrt{s} = 1800$ GeV
$\langle N_{max} \rangle$ vs. E_T^{lead}, $\sqrt{s} = 1800$ GeV
$\langle N_{min} \rangle$ vs. E_T^{lead}, $\sqrt{s} = 1800$ GeV
Swiss Cheese p_T^{sum} vs. E_T^{lead} (2 jets), $\sqrt{s} = 1800$ GeV
$\langle p_T^{max} \rangle$ vs. E_T^{lead}, $\sqrt{s} = 630$ GeV
$\langle p_T^{min} \rangle$ vs. E_T^{lead}, $\sqrt{s} = 630$ GeV
$\langle p_T^{diff} \rangle$ vs. E_T^{lead}, $\sqrt{s} = 630$ GeV
Swiss Cheese p_T^{sum} vs. E_T^{lead} (2 jets), $\sqrt{s} = 630$ GeV

D0 Run II dijet angular correlations[15]
Dijet azimuthal angle, $p_T^{max} \in [75, 100]$ GeV
Dijet azimuthal angle, $p_T^{max} \in [100, 130]$ GeV
Dijet azimuthal angle, $p_T^{max} \in [130, 180]$ GeV
Dijet azimuthal angle, $p_T^{max} > 180$ GeV
CDF Run II minimum bias[16]
$\langle p_T \rangle$ of charged particles vs. N_{ch}, $\sqrt{s} = 1960$ GeV
CDF Run I Z p_T[17]
$\frac{d\sigma}{dp_T^Z}$, $\sqrt{s} = 1800$ GeV

Parameters in AMBT1

Parameter	Related model	MC09c value	scanning range	AMBT1 value
PARP(90)	MPI (energy extrapolation)	0.2487	0.18 – 0.28	0.250
PARP(82)	MPI ($p_T^{\min}$)	2.31	2.1 – 2.5	2.292
PARP(84)	MPI matter overlap (core size)	0.7	0.0 – 1.0	0.651
PARP(83)	MPI matter overlap (fraction in core)	0.8	fixed	0.356
PARP(78)	CR strength	0.224	0.2 – 0.6	0.538
PARP(77)	CR suppression	0.0	0.25 – 1.15	1.016
PARP(93)	Primordial $k_\perp$	5.0	fixed	10.0
PARP(62)	ISR cut-off	1.0	fixed	1.025

Roberto Di Nardo – University & INFN Tor Vergata

η for K^0_s, Λ and $\bar{\Lambda}$ candidates

➢No Correction for detector effect applied

Candidates definitions

➢ $|M(K_s)-M(K_{PDG})|<20$ MeV

➢ $|M(\Lambda)-M(\Lambda_{PDG})|<7$ MeV

➢**MC consistent with data within 10%**

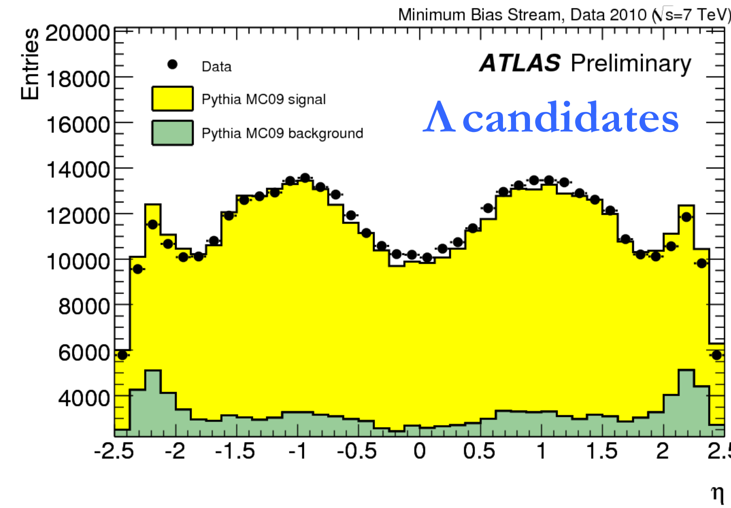

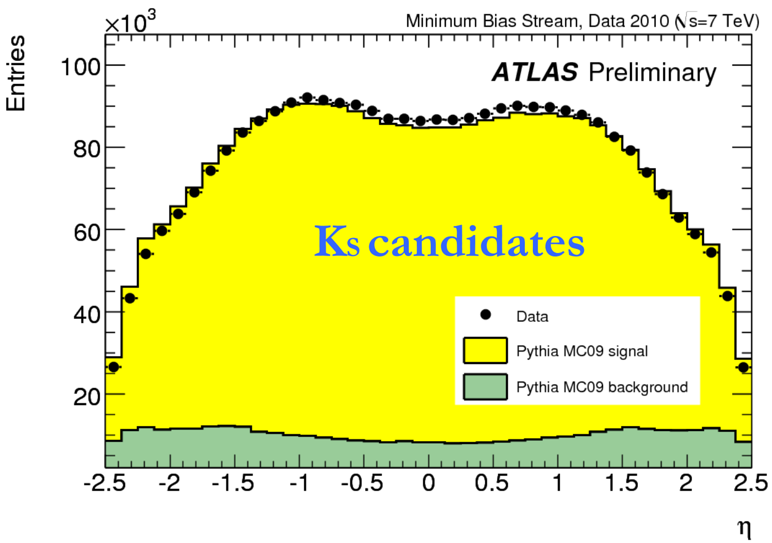

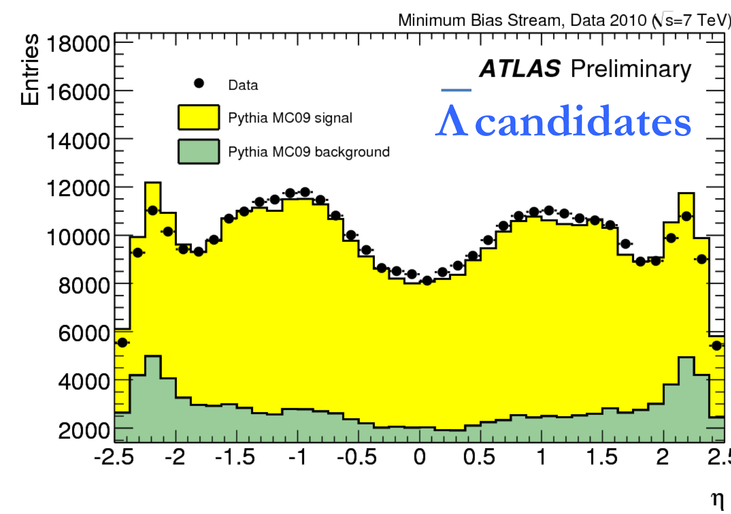

Roberto Di Nardo – University & INFN Tor Vergata

Proper decay time for K^0_s , Λ and $\bar{\Lambda}$

- No Correction for detector effect applied

Candidates definitions

- $|M(K_s)-M(K_{PDG})|<20$ MeV
- $|M(\Lambda)-M(\Lambda_{PDG})|<7$ MeV

- MC in good agreement with data
  - Worts in background dominated region for Λ and $\bar{\Lambda}$

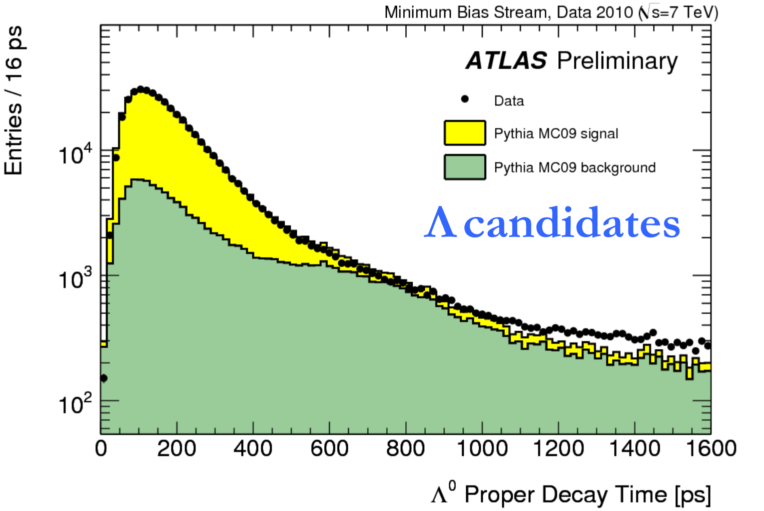

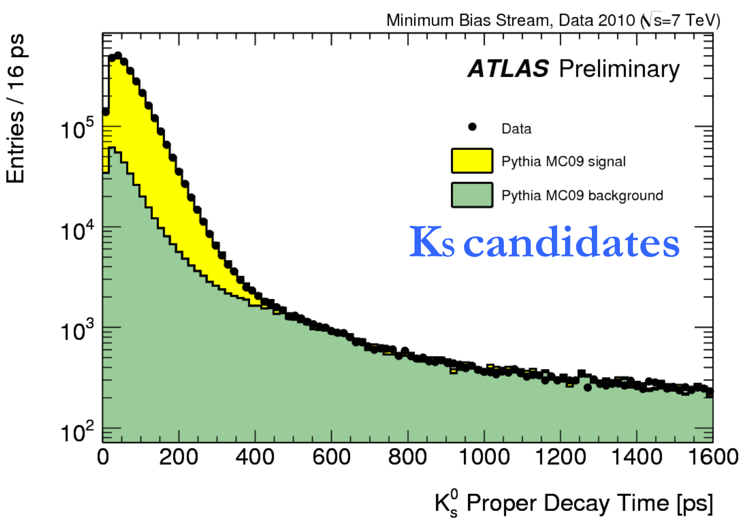

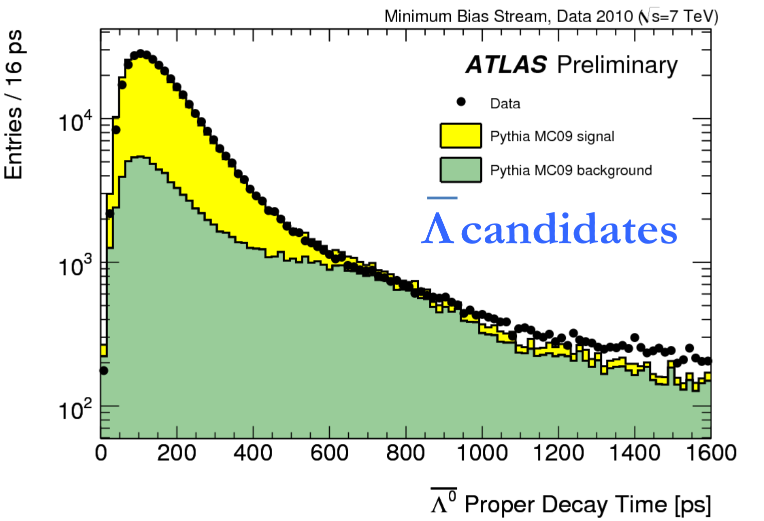

Roberto Di Nardo – University & INFN Tor Vergata

Multiplicity vs √s

- Data at different c.m.e. (@ 0.9, 2.36 and 7 TeV) have been used

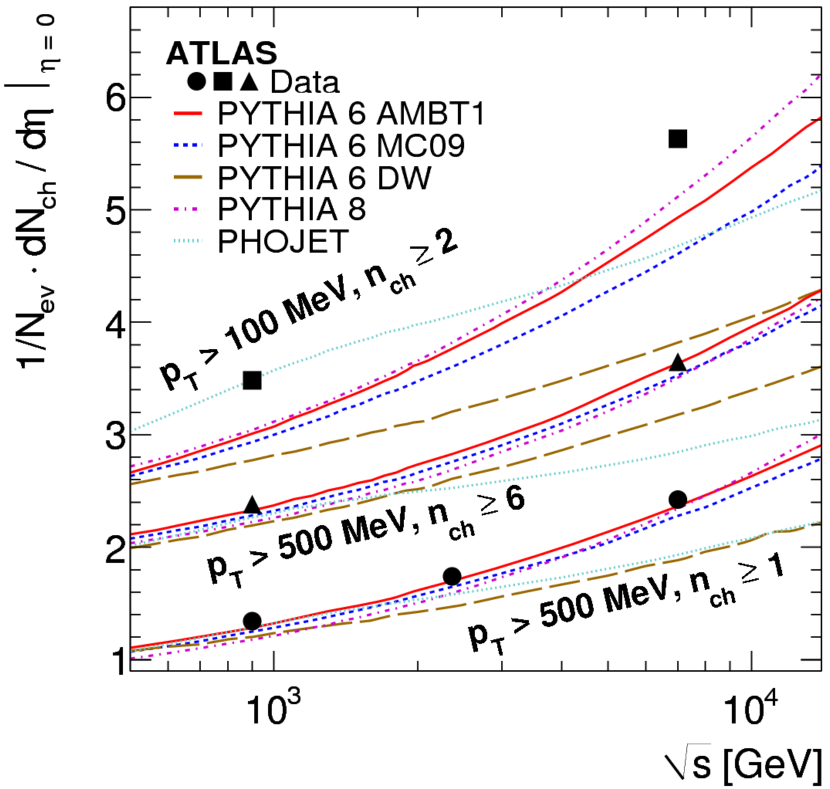

- p_T>100 MeV
  - Models underestimate the particle multiplicity
- p_T>500 MeV
  - Better Agreement for AMBT1

- no model dependent correction applied (well-defined phase-space and no correction back to a particular component (e.g. NSD))